Pergamon

Geochimica et Cosmochimica Acta, Vol. 66, No. 12, pp. 2091–2098, 2002
Copyright © 2002 Elsevier Science Ltd
Printed in the USA. All rights reserved
0016-7037/02 $22.00 + .00

PII S0016-7037(02)00906-7

Possible implications of modal mineralogy for melting in mantle lherzolites

ROBERT W. LUTH*
Department of Earth and Atmospheric Sciences, University of Alberta, Edmonton, Alberta T6G 2E3, Canada

(*Received June* 1, 2001; *accepted in revised form March* 5, 2002)

Abstract—The melting reaction at the solidus of mantle peridotite is commonly peritectic in nature, with liquid and one or more solid phases produced upon melting. In some situations, one of the phases participating on the reactant side of the reaction is present in low abundance. This article explores the possible effects of the low abundance of a reactant phase on the melting behavior of mantle peridotite.

For example, spinel lherzolite begins to melt via the peritectic reaction, clinopyroxene + orthopyroxene + spinel = olivine + liquid in the ~1- to 2-GPa pressure range. In natural spinel lherzolites, spinel is a modally minor mineral and may be infrequently in contact with both clinopyroxene and orthopyroxene. If these mutual contacts are insufficient to generate an interconnected melt, then significant melting may not occur until a combination of minerals that are modally abundant and in contact begin to melt. This scenario could have implications for the physical process of melting and for the timing of formation of an interconnected melt network and separation of the melt from the residue.

To begin to investigate this possibility, the spatial relationships between the constituent minerals in two fertile spinel lherzolites were determined by elemental mapping with the electron microprobe. Olivine, orthopyroxene, and clinopyroxene are of similar size, whereas the spinel was smaller and interstitial. Spinel and clinopyroxene are frequently in contact, but mutual contacts of spinel, clinopyroxene, and orthopyroxene are rare. Because of the changes in modal mineralogy anticipated for these lherzolites with increasing temperature, these mutual contacts will be even less common at the solidus. Therefore, an interconnected, potentially extractable, melt may not occur by the solidus spinel + orthopyroxene + clinopyroxene melting reaction. *Copyright © 2002 Elsevier Science Ltd*

1. INTRODUCTION

There is general consensus that basaltic magmas are produced by volatile-poor partial melting of lherzolite in the Earth's mantle. Melting of lherzolite containing carbonate or hydrous phases produces at least part of the compositional spectrum of volatile-bearing, mantle-derived magmas, such as carbonatites, kimberlites, and lamprophyres. Decades of experimental phase equilibrium studies on both basalts and peridotites, under a variety of P, T, $X_{volatile}$ conditions, have provided fundamental constraints on these magmatic processes, as have trace element and isotopic studies of mantle-derived magmas. Most of what we know about the thermodynamics and chemistry of melting in the mantle is from experiments on finely powdered natural and synthetic samples. The fine grain size of the powders ensures a high probability of intergrain contact between reactant minerals and improves the potential for achieving equilibrium.

One aspect of the melting process that has been relatively unexplored is the effect of modal mineralogy on the initiation of melting. In particular, solidus melting reactions for lherzolite in a variety of systems, both volatile absent and volatile present, have as a reactant phase a mineral that may be present in the rock in low abundance (Table 1). For lherzolite containing either carbonate or mica, the volatile-bearing phase is a reactant, but the abundance of such a phase is poorly constrained, depending on the process or processes that enriched the lherzolite in volatiles. For both garnet and spinel lherzolite, the aluminous phase is present in low (<5%) abundance (Maaløe and Aoki, 1977). Indeed, garnet lherzolites commonly have less clinopyroxene than garnet (Maaløe and Aoki, 1977). Clustering of these minerals (Cox et al., 1987), however, may aid in overcoming the problem of their low modal abundance and allow melting by reactions involving clinopyroxene and garnet (Table 1). In addition, the high solidus temperatures of garnet lherzolite (Walter, 1998, and references therein) would normally require the presence of volatiles for melting to occur, with the attendant uncertainties on the modal abundance of a volatile-bearing phase (see above). The volatile-absent melting of spinel lherzolites is better constrained, is relevant to basalt petrogenesis at divergent plate boundaries, and provides an illustrative example of the possible consequences of this complication on melting behavior.

For spinel lherzolites, a melting reaction of the form cpx + opx + sp = ol + liq has been proposed from studies on natural lherzolites at 1.0 to 1.5 GPa, and from studies on model systems at similar pressures (Table 1). Melt would form by this reaction where orthopyroxene, clinopyroxene, and spinel meet. This requirement becomes problematic if one of the minerals is modally scarce. Natural spinel lherzolites, even fertile ones, contain <15% clinopyroxene and <3% spinel (Table 2; Maaløe and Aoki, 1977). Maaløe (1981, 1982) recognized that the requirement for the reactant minerals to be in physical contact, coupled with the modal abundance of the minerals, limits the initial amount of melt that would be produced, and he proposed that there would be a threshold melt fraction, below which melt exists in isolation and above which the melt forms an interconnected melt network. He calculated this threshold melt fraction to be on the order of 10 to 20%. His analysis,

---

* Author to whom correspondence should be addressed (robert.luth@ualberta.ca).

Table 1. Near-solidus melting reactions for lherzolite.[a]

P (GPa)	Reaction	Reference[b]
Natural systems (volatile free)		
1.0	0.78 cpx + 0.27 opx + 0.05 sp = 1 liq + 0.10 ol	PWJ00
1.0–1.2	0.82 cpx + 0.40 opx + 0.08 sp = 1 liq + 0.30 ol	KG92
1.5	0.83 cpx + 0.33 opx + 0.08 sp = 1 liq + 0.24 ol	R98
1.5	0.58 cpx + 0.61 opx + 0.001 sp = 1 liq + 0.19 ol	R98
>2	x cpx + y ol + z gar = liq + w opx	K97
3	0.08 ol + 0.81 cpx + 0.30 gar = 1 liq + 0.19 opx	W98
Model systems (volatile free)		
CaO-MgO-Al_2O_3-SiO_2-Na_2O		
0.7	0.25 opx + 0.27 cpx + 0.53 pl = 1 liq + 0.05 ol	W95
1.3	0.42 ol + 0.97 pl = 1 liq + 0.22 opx + 0.06 cpx + 0.11 sp	W95
1.7	0.09 opx + 0.99 cpx + 0.14 sp = 1.0 liq + 0.22 ol	W95
2.0	1.27 cpx + 0.13 sp = 1.0 liq + 0.27 opx + 0.13 ol	W95
CaO-MgO-Al_2O_3-SiO_2-FeO		
1.0	0.20 opx + 0.40 cpx + 0.40 pl = 1 liq + 0.01 ol	GP00
1.2	24 ol + 27 pl = 1 liq + 4 opx + 36 cpx + 10 sp	GP00
1.7	0.10 opx + 0.99 cpx + 0.12 sp = 1 liq + 0.20 ol	GP00
2.0	1.08 cpx + 0.11 sp = 1 liq + 0.15 ol + 0.04 opx	GP00
2.7	1.33 cpx + 0.12 sp = 1 liq + 0.07 ol + 0.38 opx	GP00
1.3	0.26 opx + 0.90 cpx + 0.14 sp = 1 liq + 0.29 ol	—[c]
1.9	0.01 opx + 1.04 cpx + 0.11 sp = 1 liq + 17 ol	—[c]
Model systems (volatile-bearing)		
K_2O-CaO-MgO-Al_2O_3-SiO_2-H_2O		
<2.7	phlog + opx + cpx = ol + sp + liq	MB73
>2.7	phlog + opx + cpx = ol + gar + liq	MB73
CaO-MgO-Al_2O_3-SiO_2-CO_2		
3–4	x dmt + y opx + z gt = liq + a ol + b cpx	DP98
5–6	x mst + y cpx = liq + a ol + b gar + c opx	DP98
7	x mst + y cpx + z gt = liq + a ol + b opx	DP98

[a] cpx = clinopyroxene; opx = orthopyroxene; sp = spinel; liq = liquid; ol = olivine; gar = garnet; pl = plagioclase; phlog = phlogopite; dmt = dolomitic carbonate; mst = magnesite-rich carbonate.

[b] PWJ00 = Pickering-Witter and Johnston (2000); KG92 = Kinzler and Grove (1992); R98 = Robinson et al. (1998) first reaction for Tinaquillo lherzolite, second for "fertile" MPY lherzolite; K97 = Kinzler (1997); W98 = Walter (1998); W95 = Walter et al. (1995); GP00 = Gudfinnsson and Presnall (2000); MB73 = Modreski and Boettcher (1973); DP98 = Dalton and Presnall (1998) (see their table 4 for stoichiometric coefficients).

[c] Calculated by the author with the data of GP00 via the technique outlined in W95.

although taking into account the low modal abundance of spinel and clinopyroxene, assumed that melting was eutectoid and required mutual contact of olivine, orthopyroxene, clinopyroxene, and spinel.

The purposes of this contribution are to document the spatial relationship of spinel, clinopyroxene, and orthopyroxene in two selected spinel lherzolites, to explore how the modal abundance of these minerals would change as temperature increases to the solidus, and finally to outline the possible implications on melting processes. I suggest that the low incidence of spinel in contact with both clinopyroxene and orthopyroxene prohibits formation of an interconnected melt network at the solidus, and melting sufficient to form this network occurs only at higher temperatures, where melting at clinopyroxene + spinel contacts produces melt. At this stage, once an interconnected melt network forms, there may be a cascade effect, with a dramatic increase in melt proportion because of chemical communication through the melt network, that allows belated achievement of the true solidus melting reaction. This type of overstepping of the melting reaction was suggested previously to be of potential importance in peridotite melting (Rubie and Brearley, 1990).

Table 2. Modal mineralogy of spinel lherzolites from Maaløe and Aoki (1977).

Mineral	vol%	wt% (average)
Olivine	65–90	66.7
Orthopyroxene	5–20	23.7
Clinopyroxene	3–14	7.8
Spinel	0.2–3	1.73

2. MODAL MINERALOGY OF SPINEL LHERZOLITES

For this study, samples from the West Kettle River, British Columbia, Canada locality (Fujii and Scarfe, 1982), were selected. The whole-rock major, trace, and Sr, Nd isotopic geochemistry of these samples were reported by Xue et al. (1990). Walter (1998) determined the phase equilibria of one of these samples, KR-4003, at 3 to 7 GPa because it is a reasonable approximation of primitive, undepleted mantle. Table 3 compares the compositions of these two spinel lherzolites with various estimates for primitive undepleted mantle. Of the two, KR-4003 is the best proxy for primitive mantle and is very similar to KLB-1 (Takahashi, 1986). KR-4005 is somewhat depleted, based on its higher Mg# (molar Mg/(Mg + Fe)) and lower CaO and Al_2O_3 compared with KR-4003.

Combining the whole-rock major-element composition of these samples (Table 3) and the composition of the constituent

Table 3. Composition of Kettle River samples and estimates of primitive upper mantle.[a]

wt%	1	2	3	KLB-1	KR-4003	KR-4005
SiO_2	45.10	45.96	45.13	44.48	44.92	45.13
TiO_2	0.00	0.18	0.22	0.16	0.12	0.09
Al_2O_3	3.30	4.06	3.96	3.59	4.26	4.03
Cr_2O_3	0.00	0.00	0.00	0.00	0.41	0.4
FeO	8.00	7.54	7.82	8.10	8.02	8.13
MnO	0.00	0.13	0.13	0.12	0.13	0.14
MgO	38.10	37.78	38.30	39.22	37.34	38.21
CaO	3.10	3.21	3.50	3.44	3.45	3.36
Na_2O	0.00	0.33	0.33	0.30	0.22	0.19
K_2O	0.00	0.03	0.00	0.02	0.09	0.08
Total	97.6	99.23	99.39	99.43	98.96	99.76
CaO/Al_2O_3	0.94	0.79	0.88	0.97	0.81	0.83
Mg#	0.895	0.899	0.897	0.896	0.893	0.893

[a] 1 = pyrolite (Ringwood, 1979); 2 = LoSiMag mantle (Hart and Zindler, 1986); 3 = Least-depleted xenolith model (Jagoutz et al., 1979). KLB-1 composition is from Takahashi (1986), and KR-4003 and KR-4005 compositions are from Xue et al. (1990).

minerals (Table 4) allows calculation of the modal mineralogy (Table 5). Comparing the calculated modal mineralogy with the ranges of Maaløe and Aoki (1977) (Table 2) demonstrates that these samples are not anomalous in their abundance of either spinel or clinopyroxene.

3. SPATIAL RELATIONSHIP OF CONSTITUENT MINERALS

To determine the spatial arrangement of minerals in these samples, polished thin sections were mapped with the JEOL 8900R electron microprobe in the Department of Earth and Atmospheric Sciences, University of Alberta. WDS maps of Mg, Ca, and Fe, and an EDS map of Si abundances were obtained simultaneously on each thin section (Fig. 1). These maps were combined in Adobe Photoshop software to show clinopyroxene, spinel, and orthopyroxene as different shades of gray (Fig. 2). The white "background" represents the dominant mineral, olivine. One aspect that is lost during the image processing is an accurate depiction of grain boundaries in the monomineralic areas.

In both samples, spinel grains in contact with both orthopyroxene and clinopyroxene are in the minority (2 of 14 in KR-4003; 5 of 21 in KR-4005b). If direct contact of spinel, orthopyroxene, and clinopyroxene is required for melting to occur at the solidus, not all of these spinels could participate. This conclusion must be taken with the caveat that these sections are representative and the third phase does not contact the other two either above or below the plane of the section. If these sections are not representative, it is surprising that they both fail in the same sense, with fewer sp + opx + cpx contacts.

More common are instances where spinel contacts olivine and another mineral, not surprising given the modal abundance of olivine. For example, sp + cpx (+ol) contacts are considerably more common (9 of 14 in KR-4003; 7 of 21 in KR-4005) than are the sp + cpx + opx contacts.

4. DISCUSSION

Any discussion of these results must be done with the explicit recognition that these results are preliminary; a statistically valid sampling would require many more samples and serial sectioning of each sample to obtain a better representation of the three-dimensional texture of each sample. Such an

Table 4. Major-element compositions of minerals from Kettle River spinel lherzolites and of minerals from solidus experiment 43 of Robinson et al. (1998).

	Olivine			Orthopyroxene			Clinopyroxene			Spinel		
Element	KR-4003	KR-4005	Robinson	KR-4003	KR-4005	Robinson	KR-4003	KR-4005	Robinson	KR-4003	KR-4005	Robinson
SiO_2	39.804	40.14	41.50	54.62	54.44	53.70	50.64	50.74	49.40	0.07	0.05	1.32
TiO_2	0.017	0.00	0.01	0.12	0.22	0.27	0.97	1.05	1.02	0.36	0.32	0.32
Al_2O_3	0.016	0.03	0.16	4.82	5.22	7.60	7.76	8.07	12.50	57.69	58.24	59.2
Cr_2O_3				0.28	0.28	0.44	0.66	0.65	0.20	8.47	7.84	7.5
FeO	9.849	10.10	0.05	6.61	6.59	5.25	3.55	3.46	3.89	11.46	11.43	8.75
MnO	0.124	0.14	10.40	0.13	0.13	ND[a]	0.09	0.09	ND	0.11	0.10	ND
MgO	49.606	49.49	47.70	32.81	32.39	30.50	16.22	15.64	16.20	21.16	21.11	22.7
CaO	0.108	0.11	0.25	0.72	0.84	2.17	18.69	18.97	15.40	0.01	0.01	0.07
Na_2O				0.10	0.11	0.18	1.21	1.30	1.42	0.01	0.00	0.11
ZnO										0.08	0.04	ND
NiO	0.348	0.37	0.03	0.11	0.10	ND	0.05	0.05	ND	0.38	0.40	ND
Total	99.872	100.38	100.1	100.31	100.32	100.11	99.84	100.02	100.03	99.78	99.54	99.97

[a] ND = not determined.

Table 5. Calculated modal mineralogy for Kettle River spinel lherzolites.

Mineral	KR-4003	KR-4005
ol	48.1	52.2
opx	32.1	29.7
cpx	17.1	16.0
sp	2.7	2.1

extensive study is unlikely to provide additional insight into this problem because there is a fundamental limitation in applying these results directly to mantle melting. This limitation is that all such xenolith samples last equilibrated at temperatures well below their solidus temperature. Two-pyroxene thermometry (Wells, 1977) gives equilibration temperatures of 1079°C and 1057°C for KR-4003 and KR-4005, respectively. Solidus temperatures for mantle lherzolite are ~1250°C at 1 GPa and ~1370°C at 2 GPa (cf. review by Hirschmann, 2000). The modal mineralogy of these samples will change with increasing temperature. A rigorous evaluation of this change would require a thermodynamically based model of the subsolidus phase equilibria of peridotite that considers explicitly the effects of important minor elements such as Cr and Ti as well as major elements. In the absence of such a model, some insight may be gained by comparing the compositions of the minerals in the xenoliths with those from solidus experiments at 1.5 GPa (Robinson et al., 1998) (Table 4). The major compositional effects of increasing temperature are to increase the alumina

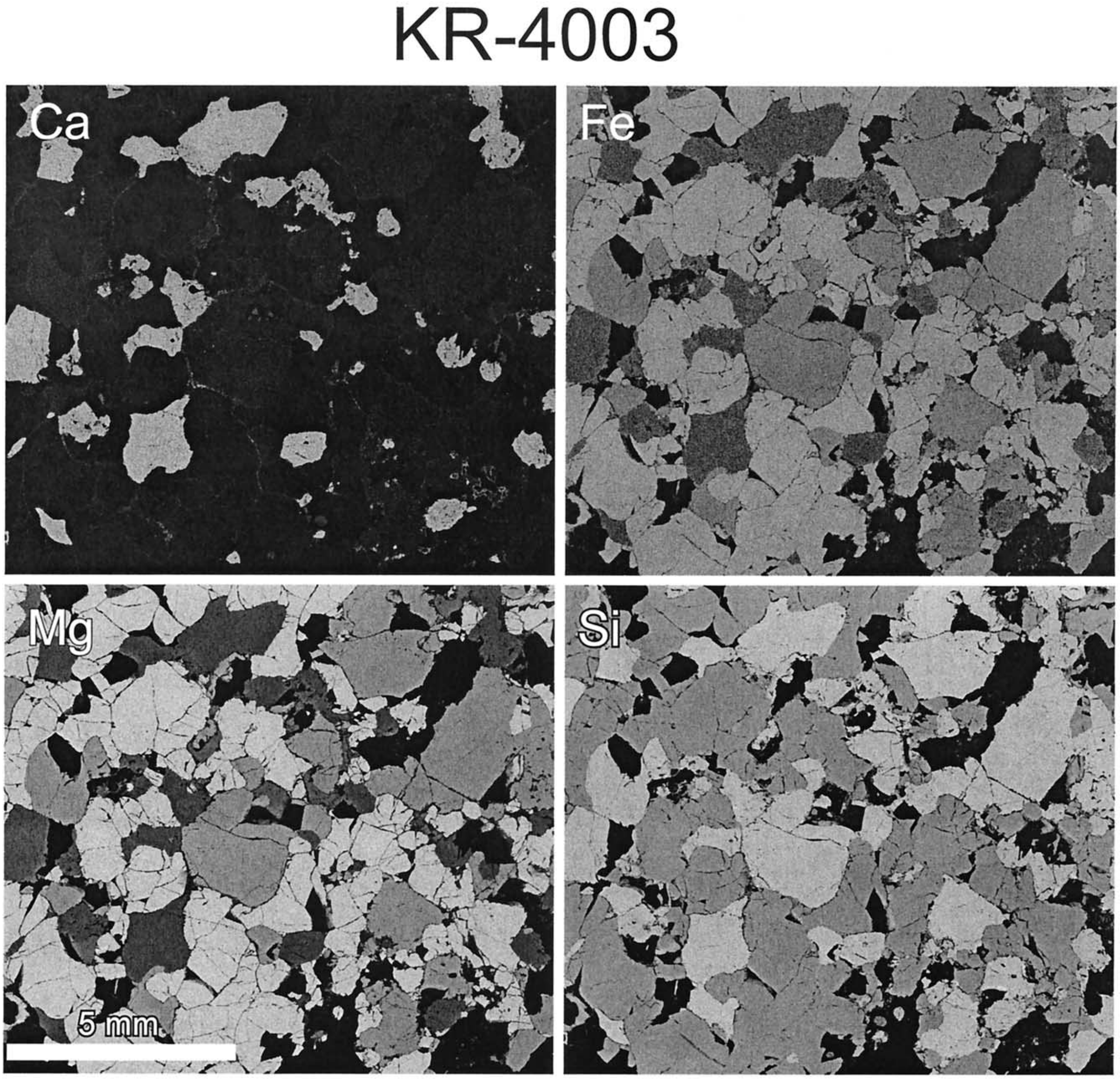

Fig. 1. Element maps of a thin section of KR-4003.

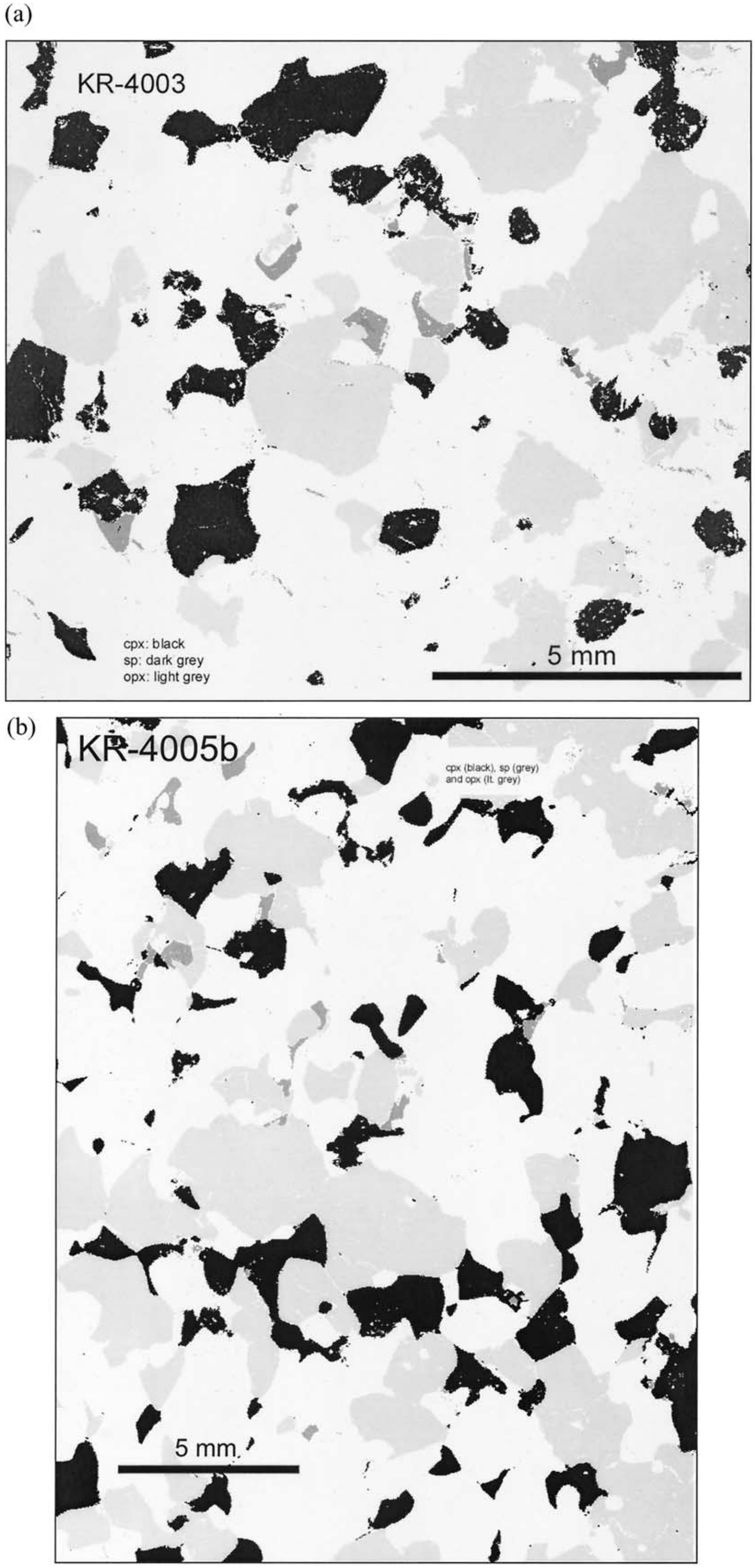

Fig. 2. Processed maps of KR-4003 (a) and KR-4005 (b) showing spatial relationships of cpx, sp, and opx. White is olivine.

Table 6. Hypothetical solidus modal mineralogy for Kettle River spinel lherzolites.

Mineral	KR-4003	KR-4005
ol	54.9	57.3
opx	22.7	21.3
cpx	22.2	21.4
sp	0.1	<0.1

content of both pyroxenes, and to decrease the calcium content of the clinopyroxene (cf. Walter, 1999). As a first approximation, the mineral compositions of Robinson et al. (1998) are combined with the bulk composition of the Kettle River lherzolites to calculate hypothetical modal mineralogies at the solidus (Table 6). Comparing Tables 5 and 6, the proportions of clinopyroxene and olivine increase with increasing temperature at the expense of orthopyroxene and spinel. The marked decrease in the amount of spinel could aggravate the problem of few sp + opx + cpx contacts. Therefore, the mutual contact results from the natural samples should be considered a "best-case" scenario for lherzolite at its solidus.

For the melting reaction cpx + sp + opx = ol + liq, the limited number of cpx + sp + opx contacts observed in the natural spinel lherzolites poses the question of whether sufficient melt could be produced by this reaction to form an interconnected network. The answer to this question depends on (1) the validity of this solidus melting reaction, (2) the amount of melt produced by this reaction, and (3) the melt fraction required to form an interconnected network. Let us consider each of these in turn.

4.1. Nature of the Melting Reaction

Table 1 summarizes solidus melting reactions inferred for spinel lherzolites. There is a 0.5-GPa pressure range over which the cpx + opx + sp = ol + liq reaction appears to describe melting at the solidus in natural spinel lherzolites. Walter et al. (1995) argue that the determination of melting reactions in these studies may accurately describe the melting reaction over the first several percent melt generated, but do not describe melting reaction *at* the solidus accurately. They argue that the melting reaction at the solidus is better inferred from calculated reactions that are based on model system experiments, where the variance is lower and the melt compositions are better constrained. On the bases of data from the CaO-MgO-Al_2O_3-SiO_2-Na_2O system (Walter and Presnall, 1994), they determine a melting reaction of the form cpx + sp = liq + ol + opx at $>$ 1.7 GPa in the spinel lherzolite stability field. They found the cpx + sp + opx = ol + liq reaction at 1.7 GPa, but did not present results for lower pressures within the spinel lherzolite field. In contrast, the study of Gudfinnsson and Presnall (2000) of the CaO-MgO-Al_2O_3-SiO_2-FeO system supports a broader pressure range for the cpx + sp + opx solidus melting reaction (Table 1), with the cpx + sp reaction again occurring at higher pressure. Changes in the solidus melting reaction with depth implies the significance of the constraint imposed by the low abundance of spinel will depend on the depth at which the solidus temperature is crossed by upwelling mantle, which in turn depends on the mantle potential temperature. Given the data in hand, however, the cpx + sp + opx = ol + liq reaction appears to describe the solidus melting reaction over a significant pressure interval in the spinel lherzolite stability field.

4.2. Amount of Melt Produced

The amount of melt produced by the solidus melting reaction will depend on the stoichiometry of the reaction, as well as on the modal abundance and composition of the reactant minerals. To illustrate the combined effect of the low modal abundance of spinel and the dominant contribution of clinopyroxene to the solidus melting reaction, consider that the area covered by clinopyroxene in contact with both orthopyroxene and spinel in the section of KR-4003 is 0.275%. This amount of clinopyroxene would produce ~0.28 to 0.47% melt, depending on the exact stoichiometry assumed for the reaction. This estimate is probably high because of the bias induced by the low-temperature modal mineralogy of the sample. Equally significant, as pointed out by Walter et al. (1995), the minerals will not melt isochemically. Instead, there is a pronounced difference between the bulk chemistry of each phase and the composition it contributes to the melt. This implies that the compositions of the residual minerals will change rapidly once melting starts, which would tend to limit the amount of melt produced at the solidus. This simple calculation of the amount of melt produced at the solidus until clinopyroxene is exhausted likely overestimates the amount of melt produced. Could a melt fraction of $<$0.3% be interconnected?

4.3. Melt Fraction Required for Interconnected Melt Network

A low-abundance phase will constrain melting only if there is a critical melt fraction required to form an interconnected melt network. This idea is contrary to the assertion that a melt network forms at melt fractions much less than 1% if the solid–solid–liquid dihedral angle is $<$60°, assessed on the basis of models of texturally equilibrated, equisize grains, with isotropic surface free energies (Waff and Bulau, 1979; von Bargen and Waff, 1986; Kohlstedt, 1992; Waff and Faul, 1992). The concept of a critical fluid or melt fraction, below which pores are isolated and an interconnected fluid or melt network does not exist, has been discussed by a number of authors (e.g., Toramaru and Fujii, 1986; Laporte and Watson, 1995; Faul, 1997, 2001; Wark and Watson, 1998), on the bases of both experimental and theoretical studies, and cannot be dismissed out of hand.

The uncertainty surrounding the magnitude and even the existence of a critical melt fraction revolves around questions of the following:

(1) the proportion of melt present in intergranular tubules (available to form the network) vs. other locations (Faul, 1997, 2001; Cmiral et al., 1998).

(2) the anisotropy of surface free energies, which might produce isolated melt pockets even for dihedral angles $<$60°, and a threshold of melt (e.g., 3 to 4 vol% in amphibolite) is required before the melt is interconnected (Laporte and Watson, 1995).

(3) the effects of other minerals. In particular, the effect of pyroxene on dihedral angle and melt connectivity in melt-

peridotite systems is unclear (Fujii et al., 1986; Toramaru and Fujii, 1986; von Bargen and Waff, 1988). Toramaru and Fujii's results imply interconnected melt at low melt fraction only for lherzolites with >75% olivine, although this estimate was decreased to ~63% olivine by Nakano and Fujii (1989).

Faul (2001) proposed that basaltic melt beneath divergent plate boundaries becomes sufficiently interconnected to become mobile at melt fractions above ~1%, although more volatile-rich and low-viscosity melts could segregate at 0.1% melt fraction. Fig. 1a of Faul (2001) illustrates the dramatic increase in permeability at ~1 to 2% melt fraction. This discontinuous increase in permeability distinguishes his model from previous models that assume the behavior at very low melt fractions is similar to that observed in experiments at higher melt fractions.

At present, it seems plausible that basaltic melts produced by the cpx + sp + opx melting reaction will remain isolated if present at <1%, and the limitation imposed by the low modal abundance of spinel is real.

4.4. Other Factors

The constraint on melt generation at the solidus imposed by low modal abundance of spinel might be eliminated either by deformation caused by mantle flow, if deformation encourages the formation of an interconnected melt network at lower melt fractions (Daines and Kohlstedt, 1997; Zimmerman et al., 1999), or by the presence of a preexisting melt (or fluid). A volatile-rich melt present at temperatures below the anhydrous solidus is certainly plausible in some circumstances. A number of authors, including Hirth and Kohlstedt (1996), Braun et al. (2000), and Faul (2001), argue that there is a small amount of hydrous melt present at greater depths below a shallower region of more extensive basaltic melt under divergent plate boundaries. Such a volatile-rich, low viscosity melt should achieve an interconnected network at low melt fraction more readily (Faul, 2001). Such melts may be either H_2O- or CO_2-rich, although CO_2-rich melts would freeze out upon ascent because of the "ledge" on the lherzolite + CO_2 solidus produced by the intersection of subsolidus carbonation reactions with the solidus and the attendant increase in CO_2 solubility with increasing pressure. This "ledge" occurs at ~1.8 GPa (Falloon and Green, 1989) and at ~2.7 GPa in the CaO-MgO-Al_2O_3-SiO_2-CO_2 system (Dalton and Presnall, 1998, and references therein). Such melts could exist within the spinel lherzolite stability field at temperatures below those of the anhydrous solidus. Diffusion through, or advection of, such a melt would allow reactant minerals not in physical contact to equilibrate, and would remove the constraint imposed by the low abundance of spinel in contact with both clinopyroxene and orthopyroxene. Consideration of the presence of these melts is complicated by uncertainties concerning their composition, pervasiveness, and by the dissolution of water into nominally anhydrous minerals. This later model is that favored by Hirth and Kohlstedt (1996) and Braun et al. (2000). Although the melting of hydrogen-bearing, nominally anhydrous minerals at lower temperatures than their hydrogen-free analogues is key to this model, the magnitude of this effect has not been calibrated experimentally. At present, it is unclear if this melt would be present throughout the upper mantle or whether it would affect melting in all tectonic environments.

4.5. Consequences for Melting in the Mantle

How large might this effect of modal mineralogy on mantle melting be? If the temperature of the true solidus, defined by cpx + opx + sp = liq + ol, is only a few degrees below melting reactions such as cpx + sp = ? + liq, then the overstepping of the solidus because of the modal mineralogy effect would be trivial. In the absence of pertinent data for the natural system, consider the available data from the system CaO-MgO-Al_2O_3-SiO_2. At 2 GPa, the reaction en + di + sp = liq + fo occurs at 1470°C, and the en-absent reaction di + sp = liq + fo occurs at 1485°C (Liu and Presnall, 2000). If this 15°C difference in the two melting reactions were to apply to nature, it would translate to a 25-km depth difference along a 0.6°C/km adiabat (McKenzie and Bickle, 1988). If the upwelling mantle intersects the solidus at a 50- to 70-km depth, this 25-km interval over which the mantle is above its solidus without the formation of an interconnected melt is a significant fraction of its ascent. Calculations of aggregate melts produced by polybaric melting (e.g., Walter, 1999) need to consider the effect that this delay on formation of melt would have on the depth of initiation of melting, on melt productivity during ascent (typically scaled as percent melt generated per kilometer ascent), and on the compositions of the melts produced.

Critical tests of this hypothesis will include, first, experimental verification of an interconnectivity threshold in lherzolites, and second, experimental studies designed to determine precisely the melting temperatures of opx + cpx + sp, cpx + sp, opx + cpx, etc., for mineral compositions appropriate for solidus temperatures.

Acknowledgments—This contribution is dedicated to Hatten S. Yoder Jr. in recognition of his pioneering efforts in applying experimental studies to understand the Earth. I thank C. T. Prewitt and B. Mysen for the invitation to participate in the Yoder Symposium in March 2001. This research was supported by NSERC research grants to the author. I thank the reviewers for their constructive reviews. In particular, I am grateful for the comments by Dean Presnall, whose input greatly improved this contribution.

Associate editor: M. A. Menzies

REFERENCES

Braun M. G., Hirth G., and Parmentier E. M. (2000) The effects of deep damp melting on mantle flow and melt generation beneath mid-ocean ridges. *Earth Planet. Sci. Lett.* **176,** 339–356.

Cmiral M., Fitz Gerald J. D., Faul U. H., and Green D. H. (1998) A close look at dihedral angles and melt geometry in olivine-basalt aggregates: A TEM study. *Contrib. Mineral. Petrol.* **130,** 336–345.

Cox K. G., Smith M. R., and Beswetherick S. (1987) Textural studies of garnet lherzolites: Evidence of exsolution origin from high-temperature harzburgites. In *Mantle Xenoliths* (ed. P. H. Nixon), pp. 537–550. Wiley.

Daines M. J. and Kohlstedt D. L. (1997) Influence of deformation on melt topology in peridotites. *J. Geophys. Res.* **102,** 10257–10271.

Dalton J. A. and Presnall D. C. (1998) Carbonatitic melts along the solidus of model lherzolite in the system CaO-MgO-Al_2O_3-SiO_2-CO_2 from 3 to 7 GPa. *Contrib. Mineral. Petrol.* **131,** 123–135.

Falloon T. J. and Green D. H. (1989) The solidus of carbonated, fertile peridotite. *Earth Planet. Sci. Lett.* **94,** 364–370.

Faul U. H. (1997) Permeability of partially molten upper mantle rocks from experiments and percolation theory. *J. Geophys. Res.* **102,** 10299–10311.

Faul U. H. (2001) Melt retention and segregation beneath mid-ocean ridges. *Nature* **410,** 920–923.

Fujii T. and Scarfe C. M. (1982) Petrology of ultramafic nodules from West Kettle River, near Kelowna, southern British Columbia. *Contrib. Mineral. Petrol.* **80,** 297–306.

Fujii N., Osamura K., and Takahashi E. (1986) Effect of water saturation on the distribution of partial melt in the olivine-pyroxene-plagioclase system. *J. Geophys. Res.* **91,** 9253–9259.

Gudfinnsson G. H. and Presnall D. C. (2000) Melting behaviour of model lherzolite in the system CaO-MgO-Al_2O_3-SiO_2-FeO at 0.7–2.8 GPa. *J. Petrol.* **41,** 1241–1269.

Hart S. R. and Zindler A. (1986) In search of a bulk-earth composition. *Chem. Geol.* **57,** 247–267.

Hirschmann M. M. (2000) Mantle solidus: Experimental constraints and the effects of peridotite composition. *Geochem. Geophys. Geosyst.* **1** Paper #2000GC000070. [11,012 words, 12 figures, 3 tables].

Hirth G. and Kohlstedt D. L. (1996) Water in the oceanic upper mantle: Implications for rheology, melt extraction and the evolution of the lithosphere. *Earth Planet. Sci. Lett.* **144,** 93–108.

Jagoutz E., Palme H., Baddenhausen H., Blum K., Cendales K., Dreibus G., Spettel B., Lorenz V., and Wanke H. (1979) The abundances of major, minor and trace elements in the Earth's mantle as derived from primitive ultramafic nodules. *Proceed. 10th Lunar Planet. Sci. Conf.* **10,** Vol. 2, 2031–2050.

Kinzler R. J. (1997) Melting of mantle peridotite at pressures approaching the spinel to garnet transition: Application to mid-ocean ridge basalt petrogenesis. *J. Geophys. Res.* **102,** 853–874.

Kinzler R. J. and Grove T. L. (1992) Primary magmas of mid-ocean ridge basalts. 1. Experiments and methods. *J. Geophys. Res.* **97,** 6885–6906.

Kohlstedt D. L. (1992) Structure, rheology and permeability of partially molten rocks at low melt fractions. In *Mantle Flow and Melt Generation at Mid-Ocean Ridges* (eds. J. P. Morgan, D. K. Blackman, and J. M. Sinton), pp. 103–121. American Geophysical Union Geophysical Monograph 71.

Laporte D. and Watson E. B. (1995) Experimental and theoretical constraints on melt distribution in crustal sources: The effect of crystalline anisotropy on melt interconnectivity. *Chem. Geol.* **124,** 161–184.

Liu T.-C. and Presnall D. C. (2000) Liquidus phase relations in the system CaO-MgO-Al_2O_3-SiO_2 at 2.0 GPa: Applications to basalt fractionation, eclogites, and igneous sapphirine. *J. Petrol.* **41,** 3–20.

Maaløe S. (1981) Magma accumulation in the ascending mantle. *J. Geol. Soc. Lond.* **138,** 223–236.

Maaløe S. (1982) Geochemical aspects of permeability controlled partial melting and fractional crystallization. *Geochim. Cosmochim. Acta* **46,** 43–57.

Maaløe S. and Aoki K.-I. (1977) The major element composition of the upper mantle estimated from the composition of lherzolites. *Contrib. Mineral. Petrol.* **63,** 161–173.

McKenzie D. and Bickle M. J. (1988) The volume and composition of melt generated by extension of the lithosphere. *J. Petrol.* **29,** 625–679.

Modreski P. J. and Boettcher A. L. (1973) Phase relationships of phlogopite in the system K_2O-MgO-CaO-Al_2O_3-SiO_2-H_2O to 35 kilobars: A better model for micas in the interior of the Earth. *Am. J. Sci.* **273,** 385–414.

Nakano T. and Fujii N. (1989) The multiphase grain control percolation: Its implication for a partially molten rock. *J. Geophys. Res.* **94,** 15653–15661.

Pickering-Witter J. and Johnston A. D. (2000) The effects of variable bulk composition on the melting systematics of fertile peridotitic assemblages. *Contrib. Mineral. Petrol.* **140,** 190–211.

Ringwood A. E. (1979) *Origin of the Earth and Moon*. Springer-Verlag.

Robinson J. A. C., Wood B. J., and Blundy J. D. (1998) The beginning of melting of fertile and depleted peridotite at 1.5 GPa. *Earth Planet. Sci. Lett.* **155,** 97–111.

Rubie D. C. and Brearley A. J. (1990) A model for rates of disequilibrium melting during metamorphism. In *High-Temperature Metamorphism and Crustal Anatexis* (eds. J. R. Ashworth and M. Brown), pp. 57–86. Unwin Hyman.

Takahashi E. (1986) Melting of a dry peridotite KLB-1 up to 14 GPa: Implications on the origin of peridotitic upper mantle. *J. Geophys. Res.* **91,** 9367–9382.

Toramaru A. and Fujii N. (1986) Connectivity of melt phase in a partially molten peridotite. *J. Geophys. Res.* **91,** 9239–9252.

von Bargen N. and Waff H. S. (1986) Permeabilities interfacial areas and curvatures of partially molten systems: Results of numerical computations of equilibrium microstructures. *J. Geophys. Res.* **91,** 9261–9276.

von Bargen N. and Waff H. S. (1988) Wetting of enstatite by basaltic melt at 1350°C and 1.0- to 2.5-GPa pressure. *J. Geophys. Res.* **93,** 1153–1158.

Waff H. S. and Bulau J. R. (1979) Equilibrium fluid distribution in an ultramafic partial melt under hydrostatic stress conditions. *J. Geophys. Res.* **84,** 6109–6114.

Waff H. S. and Faul U. H. (1992) Effects of crystalline anisotropy on fluid distribution in ultramafic partial melts. *J. Geophys. Res.* **97,** 9003–9014.

Walter M. J. (1998) Melting of garnet peridotite and the origin of komatiite and depleted lithosphere. *J. Petrol.* **39,** 29–60.

Walter M. J. (1999) Comments on "Mantle melting and melt extraction processes beneath ocean ridges: Evidence from abyssal peridotites" by Yaoling Niu. *J. Petrol.* **41,** 1187–1193.

Walter M. J. and Presnall D. C. (1994) Melting behavior of simplified lherzolite in the system CaO-MgO-Al_2O_3-SiO_2-Na_2O from 7 to 35 kbar. *J. Petrol.* **35,** 329–359.

Walter M. J., Sisson T. W., and Presnall D. C. (1995) A mass proportion method for calculating melting reactions and application to melting of model upper mantle lherzolite. *Earth Planet. Sci. Lett.* **135,** 77–90.

Wark D. A. and Watson E. B. (1998) Grain-scale permeabilities of texturally equilibrated, monomineralic rocks. *Earth Planet. Sci. Lett.* **164,** 591–605.

Wells P. R. A. (1977) Pyroxene thermometry in simple and complex systems. *Contrib. Mineral. Petrol.* **62,** 129–139.

Xue X., Baadsgaard H., Irving A. J., and Scarfe C. M. (1990) Geochemical and isotopic characteristics of lithospheric mantle beneath West Kettle River, Br. Columbia: Evidence from ultramafic xenoliths. *J. Geophys. Res.* **95,** 15879–15891.

Zimmerman M. E., Zhang S., Kohlstedt D. L., and Karato S.-I. (1999) Melt distribution in mantle rocks deformed in shear. *Geophys. Res. Lett.* **26,** 1505–1508.